Recovery Modeling for OSB Strand Production from Hollow Bamboo Culms

Kate E. Semple,[a] and Gregory D. Smith [b,*]

Current methods of reducing giant Moso bamboo (*Phyllostachys pubescens* Mazel) to elements for composite manufacture are often inefficient and waste valuable biomass. This study employed geometric modelling to analyze and optimize the recovery of strands for oriented strand board manufacture. Three geometric models for calculating the numbers of strands, their widths, and their distribution based on culm diameter, wall thickness, target strand thickness, and flitch size were developed to determine an optimum slicing configuration. Real strands were produced by a disk flaker at the model strand thickness of 0.65 mm. Optimum configuration for the maximum number of usable strands per culm was from splitting culms into quarters, tight stacking, and radial slicing through the culm wall, which produced 37% more 'usable' strands 10 mm to 30 mm in width, fewer fines, and fewer excessively wide strands. Proportions of real strands fell into three size classes: < 10 mm, 10 mm to 30 mm, and > 30 mm, and closely matched modelled predictions. A slightly bimodal strand width frequency distribution observed from stranding full rounds was reflected in the distribution of the model strands calculated from slicing a full round into 0.65 mm increments.

Keywords: Bamboo; Oriented Strand Board; Production Efficiency; Geometric modeling

*Contact information: a: FP Innovations, 2665 East Mall, Vancouver, BC, V6T 1Z4, Canada; b: University of British Columbia Department of Wood Science, 2900-2424 Main Mall, Vancouver, BC, V6T 1Z4, Canada; *Corresponding Author: Greg.Smith@ubc.ca*

INTRODUCTION

Bamboos are giant grasses belonging to the family Poaceae/Graminaceae with approximately 1,225 known species (Austin and Ueda 1972). They have been used in traditional house construction for centuries and are emerging as a significant non-wood forest resource as a result of deforestation where it grows native across the tropical and subtropical belt of Asia, Africa, and Latin America (Liese 1998; Scurlock *et al*. 2000; Fu *et al.* 2001). Over one billion people live in dwellings built using bamboo materials (De Flander and Rovers 2009). However traditional raw bamboo rounds and splits are unsuitable for more modern construction applications that use dimension lumber or composites due to their propensity for splitting and flaws, highly variable geometry, and their physical and mechanical properties within and across culms (Van der Lugt *et al.* 2006; Correal and Ramirez 2010; Harries *et al.* 2012). To overcome such problems in the case of wood resources, thin strand-based engineered wood products, such as Waferboard and Oriented Strand Board (OSB), have been developed. These products have enabled the successful conversion of small diameter, fast growing regrowth, or plantation trees into reliable construction materials with adjustable, uniform, and predicable strength

properties and dimensional stability (Lowood 1997; Moses and Prion 2004; Starke *et al.* 2010).

Many of the 'mature' conversion technologies developed for wood, such as particleboard, laminate-based composites (*e.g.* glulam) and strand-based panels, and lumber are transferable to non-wood industrial woody crop resources such as bamboo. Many laboratory studies have demonstrated that high performance strand-based panels and lumber can be produced from bamboo (*e.g.* Lee *et al.* 1996; Sumardi *et al.* 2006, 2007, 2008; Malanit *et al.* 2011; Semple *et al.* 2015a, b). However, the technological adaptation for industrial-scale production is far less developed, and there are currently very few successful examples of the commercial-scale conversion of bamboo into engineered building materials compared with wood. The conversion of small diameter, hollow bamboo resources into strand-based structural composite products is a demonstrated example of an excellent conversion option. However, transition to commercial production has been hampered by its peculiar physical and material properties. These properties pose challenges for efficient conversion into strands using slicing machinery designed exclusively for wood logs.

In recent decades, countries such as China and Columbia have successfully developed industrial cultivation and use of giant timber bamboo, the most common examples being Moso (*Phyllostachys pubescens* Mazel) and Guadua (*Guadua angustifolia* Kunth.). The small diameter (mostly less than approximately 120 mm) and limited wall thickness (mostly less than 12 mm) of hollow timber bamboo culms limits the range of processing options compared with wood logs. Also, the most mature conversion technologies for bamboo involve the manufacture of laminated composite lumber and panels from dried, milled tangential strips from the culm wall. These are time and labour-intensive to produce, waste a large amount (40% to 60%) of the costly culm biomass, and discard the most fibre-rich, strongest material located at the outer culm wall. Moso bamboo has been identified as a promising potential feedstock for OSB production in China (Fu 2007a), a far more efficient conversion and manufacturing process than laminated lumber. Conversion of bamboo culms into thinly sliced radial strands does not require removal of outer and inner wall material, and culm tissue recovery for the end-product is much higher, typically above 80%. Studies on characterizing and optimizing strand quality from Moso bamboo (Semple *et al.* 2014, 2015a,b) show that strands/fines recovery from Moso bamboo compares favorably with the proportions of strands *vs.* fines found in industrial OSB furnish produced from Aspen logs, and that Moso is much easier to process into OSB strands than Guadua. Slicing is also very fast and drying of thin strands is much faster than thick solid strips, merely minutes as opposed to weeks.

The potential has been recognized by at least one enterprise, Yunnan Yung Lifa Forest Co. Ltd., in China, which has spent several years adapting OSB technology to bamboo and recently commissioned a pilot plant to produce tough, durable bamboo OSB flooring for shipping containers (Anon 2012; Grossenbacher 2012). However, a significant bottleneck in the process is the conversion of culm stock to strands. The immediately obvious challenges for converting stranding culm stock to strands include the extremely hard, dense outer cortex of culms, over 50% of the culm volume being air-space, and the presence of dense, tough node plates. The Yunnan Yung Lifa pilot plant uses horizontal disk stranders to cut strands from green pieces that have been manually cross-cut into node-free rounds approximately 130 mm in length (Grossenbacher 2012).

Node removal is done to facilitate this and eliminate any adverse effects of nodes on strand and board quality. Such an approach allows stacking of small rounds inside larger ones, increasing the number of strands produced per machine running time. Not only is this process highly labor-intensive, it also results in significant losses in biomass recovery that can be evaluated and improved using even simple numerical modelling.

Numerical modelling (especially finite element modeling, FEM) is being increasingly applied in all fields of material science, including wood and wood-based composite materials (Wang and Lam 1998). In wood, or other lignocellulosic-based materials (*e.g.* bamboo), optimization and modeling research has focused on the prediction of the properties and behavior of the end products. Much research has focused on the predictive models for strand boards properties (including bamboo) based on adjustable input variables including wood/bamboo species (density, mechanical properties, and moisture content), strand size and geometry, orientation relative to the plane of loading, adhesive resin type and quantity, and hot pressing parameters (Triche and Hunt 1993; Wang and Lam 1998; Clouston and Lam 2002; Sumardi and Suzuki 2013; Malek *et al.* 2014; Dixon *et al.* 2017).

In contrast, there are very few published studies on the conversion stage of wood or bamboo into strands for industrial strand-based composite lumber and panels, and just two referring to the conversion of bamboo culms to strands. A short description of using a small lab-scale disk flaker to convert 130 mm long node-free half rounds of moso bamboo to strands for OSB fabrication is given in Malanit *et al.* (2011). The most detailed treatise found on stranding bamboo culms is a Ph.D. thesis by Fu (2007b) that describes what appears to be an efficient method of converting industrial quantities of bamboo poles to strands. The usually 240-cm long poles are first split into 8 sections or 'flitches' using a motorized splitting wheel commonly used in the bamboo processing industry in China. This step also removes most of the central node plate, and is followed by grinding flat the remaining node material from the inner wall to allow tight stacking. The flitches are clamped together in tight stacks of four rows by 15 to 20 flitches high, which are fed laterally against the inner knife-mounted wall of a ring flaker that cuts largely radial strands of a length determined by the spacing of the scoring knives.

Efficient industrial fabrication of OSB from bamboo in China is currently hampered by the lack of purpose-designed slicing machinery and methodology to convert bamboo poles into strands while maximizing material recovery rate. There are no published numerical models or analyses developed to better understand the efficiency of conversion of bamboo culms to thin strands. A better fundamental understanding of slicing of hollow, thick walled tubes will help in designing and producing strand conversion equipment tailored to bamboo. While variation exists in culm breakdown techniques in the bamboo industry, there is an optimum configuration by which culms should be broken down and converted to strands for any potential industrial-scale OSB production from hollow bamboo culms. This study uses geometric modelling to evaluate the strand size and recovery from four different slicing configurations for culms: whole rounds, halves, quarters, or eight narrower flitches. Hypothetically slicing rounds is less efficient in terms of strand recovery than converting them to smaller sections, but to what extent?

This study develops theoretical models for predicting the numbers of strands and the width of every strand resulting from slicing either one whole culm, two halves, four quarters, or eight narrower flitches with fixed input variables of strand thickness, culm

diameter, and wall thickness, as well as piece orientation relative to the strander knife. It will also generate theoretical strand width frequency distributions for stranding a whole culm, two halves, four quarters, or eighths, and use them to verify the shape of the actual strand width distributions from stranding real culms under similar conditions. From these procedures, it will be determined which culm break-down method is most efficient in terms of number of strands per unit culm wall area, and the strander operating time. The method that best meets the desired strand width distribution for OSB manufacture will be evaluated.

EXPERIMENTAL

Materials

Seasoned, Chinese-grown Moso bamboo culms in the largest (5") diameter range available were purchased from Canada's Bamboo World, Chilliwack, BC, Canada. These were cross-cut into 130 mm- long rounds that were re-saturated and converted to OSB strands using a 0.94-m diameter 6/36 Lab Flaker (Fig. 1) built by Carmanah Design and Manufacturing, Ltd., Vancouver, Canada. The outer section of the disk was fit with a knife housing block accommodating a 180-mm long disposable twin blade knife with a low counter-knife angle of 40° designed for stranding denser (by OSB standards) woods such as Southern Pine. The flaker was designed and built to strand small blocks of solid wood measuring up to 130 mm wide × 130 mm high × 180 mm long, which required the bamboo culms to be first cross cut into lengths no greater than 130 mm. Disposable twin blades were used and swapped for a new blade after approximately 6 h of stranding. The blade was kept lubricated with water using a small spray valve, and the culm pieces were stood on their end kept contained inside the feed drawer using a custom-fabricated plywood lid clamped over the top with a large C-clamp to prevent pieces from dislodging during cutting. Preliminary work on stranding Moso bamboo (Semple *et al*. 2014, 2015a) found that the optimum strand quality was obtained through re-saturating the culm pieces to above 130% moisture content and stacking vertically, *i.e.* slicing the culm longitudinally to a nominal target thickness of 0.65 mm (knife protrusion setting = 0.73 mm). The corresponding material feed rate was 0.47 m/sec, disk operating speed of 734 RPM, and low counter knife angle of 40°.

Fig. 1. CAE 6/36 Lab Flaker, disk rotation direction is clock-wise; inset: close up view of disposable twin blade in its housing

Culm rounds were stranded as either two intact rounds per run (feed drawer load) as shown in Fig. 2a, eight half rounds (Fig. 2b), or 18 to 22 quartered rounds (Fig. 2c). Attempting to strand the narrow flitches that resulted from dividing the culm into eighths proved difficult and impractical due to the vertical instability of the large number of unsecured tall, narrow pieces. Even for the quarters, variation in the culm wall thickness, piece width, and protruding portions of node tissue prevented the precise arrangement of the maximum number of pieces, as shown schematically in Fig. 2c.

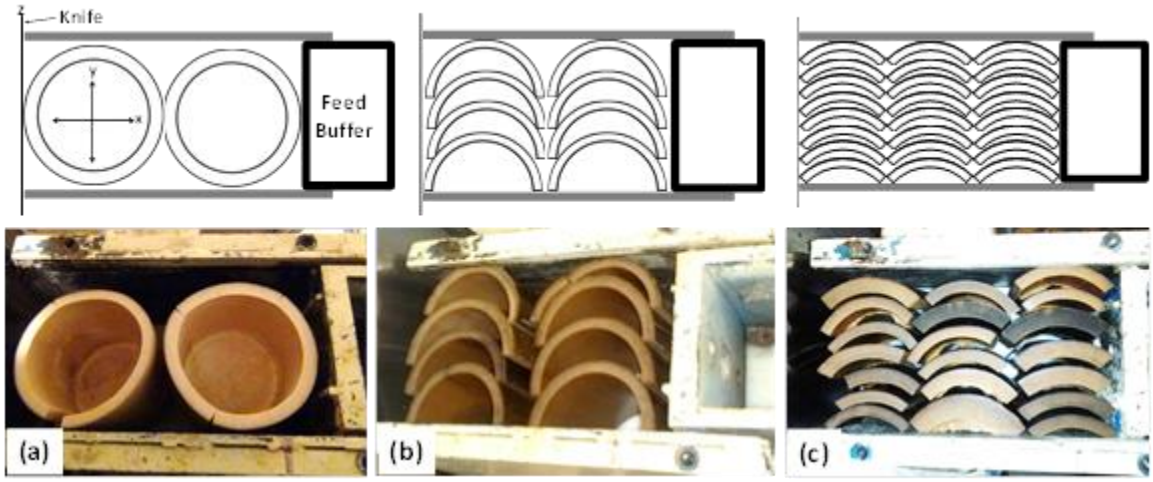

Fig. 2. Schematic (top row) and actual (bottom row) configurations for culm piece size and vertical placement in strander feed drawer: (a) whole culm rounds, (b) half rounds, and (c) quarters

Wet strands were collected from beneath the disk in a long pull-out drawer, distributed into wire baskets, and dried at 80 °C in a large convection oven (Despatch Oven Co., Minneapolis, MN, USA) overnight. Post-drying moisture content of the strands was less than 2%. Strands from the different slicing configurations were kept separate during drying, bagging, and handling. Approximately 5 kg of dried strands were

produced per configuration; for an average dry weight of 310 g per culm piece, each batch represented 16 full round equivalents requiring 8 drawer runs, 4 runs for halves, and 2 to 3 runs for quarters. From each batch of strands, approximately 12 random handfuls of strands (each approximately 30 strands) were removed and measured for width using a digital caliper. The numbers of strands measured in each case was equivalent to the total number of strands generated by the models from slicing either one whole culm round, 2 halves, or 4 quarters in 0.65 mm increments. Examples of real strands cut from whole, half, or quarter culms can be seen in Fig. 3.

Methods

Generation of strand width series

To predict frequency distributions of strand width from slicing a whole culm, two half culms, four quarter culms, or the culm round divided into eight even-sized flitches, complete lists of model strands must be compiled from four geometric models developed to calculate the width and cross-sectional area of every strand in the order as they are cut. The constants and variable parameters used in the models are given in Table 1. When developing the models, inner and outer circumferences of culms were kept circular, with wall thickness kept constant. The wall remained free of splits. The *Y*-axis of the illustrated culm piece orientations (Figs. 2a through c) was parallel to the cutting blade, and the plane of slicing was flat. Culm pieces moved towards the blade by translation along the *X*-axis only. The slicing of the culm wall was exactly longitudinal, *i.e.* through the *z*-plane as shown in Fig. 2a.

Fig. 3. Examples of real strands (1) strand from close to point *r* from slicing a half round, (2) strand from close to point *R* from slicing a full round, (3) full wall strand between points *c* and *r*, and (4) full wall strand close to *Y*-axis slicing halves or quarters

Table 1. Constant Model Input Parameters and Variables

Constants (mm)		Variables	
Outer Culm Dia. (*D*)	110.5	1. Culm sectioning	1 × whole culm 2 × half culm 4 × quarter culm 8 × eighth culm
Outer Radius (*R*)	55.25		
Wall Thickness (*w*)	11.05		
Inner Wall Dia. (*d*)	88.4		
Inner Wall Radius (*r*)	44.2	2. Strand width	
Strand Thickness (*t*)	0.65	3. Strand transverse cross-sectional area	
Strand Length (*L*)	130		

To generate model strands from slicing the whole or half culm, a schematic diagram of the whole culm round intersected with a vertical *Y*-axis and horizontal *X*-axis through point *c* is shown in Fig. 4a. All slices were made parallel to the *Y*-axis. These are the reference lines used to calculate the *Y*-axis values that correspond to points located around the perimeter of the outer and inner culm wall. Because each strand has a slightly rounded edge, the model strand width corresponds to the wider of the strands two faces, which is also the width measured on the real strands if measured with calipers.

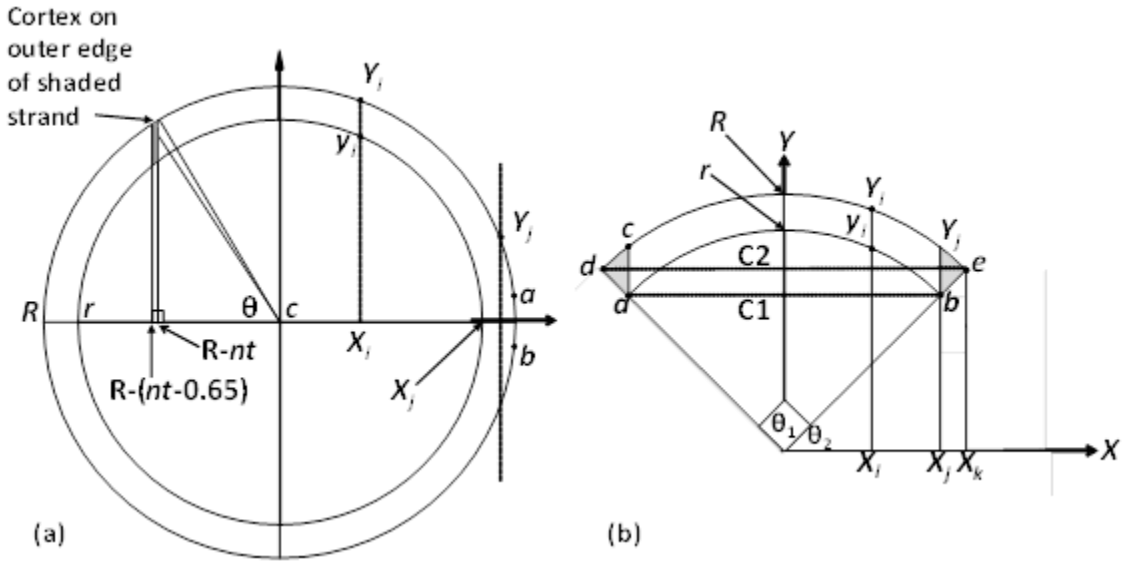

Fig. 4. Reference points for calculating strand widths from (a) whole, half culm and (b) quarters or eighth sections from the culm round

Along the horizontal *X*-axis in both directions out from point *c*, there were two outer zones of strands cut between *R* and *r*; the distance equated to culm wall thickness, 11.05 mm along the *X*-axis. Dividing this by nominal strand thickness, t = 0.65 mm, gave two symmetrical sets of 17 strands each. To generate the width of each strand in the set, the corresponding *X*-axis values (X_j) at each increment out from point *r*, were derived first: $X_{j1} = r + t$, $X_{j2} = r + 2t$, $X_{j3} = r + 3t$,…. through to strand 17 at point *R*.

The corresponding Y_j values for each point along the outer culm circumference out to point *R*, are:

$$Y_j = (R^2 - X_j^2)^{½} \quad (1)$$

The strand width equals $2Y_j$, or is equivalent to Y_j if slicing half culm rounds. Two half culms contain four sets of outer strands, totaling 68, which adds an extra 34 strands to the total number of strands generated for slicing two half rounds compared to slicing one full round.

Strands located between point *c* and *r* (Fig. 4a) ranged in width from a minimum equivalent to culm wall thickness, 11.05 mm, at the *Y*-axis to a maximum at *r*. In one whole culm, there are four symmetrical quadrants where these strands occur; *r* corresponds to the distance (44.2 mm), along the X-axis; *r* / *t* (0.65 mm per strand) gave 68 strands per quadrant, or a total of 272 strands for the four quadrants. The set of model strands is the same for one full round or two half rounds. The x-axis values are: $X_{i1} = t$, $X_{i2} = 2t$, $X_{i3} = 3t$,…. through to 68 at point *r* (44.2 mm). The corresponding Y_i and y_i values were calculated according to Eq. 2.

$$Y_i = (R^2 - X_i^2)^{½} \text{ and } y_i = (r^2 - X_i^2)^{½} \quad (2)$$

The widths of each strand are the $Y_i - y_i$ values, *e.g.* for the strand at point *c*: X_i = 0.65 mm; $Y_{i1} = (55.25^2 - 0.65^2)^{½}$, or 55.25 mm; and $y_{i1} = (44.2^2 - 0.65^2)^{½}$, or 44.19 mm; $Y_{i1} - y_{i1}$ = 11.05 mm.

The schematic diagram for slicing a quarter round rotated so that the *Y*-axis bisected the piece radially and all slices were made parallel to *Y*-axis is shown in Fig 4b. Strands between points *a* and *b* represent the entire wall thickness with the outer cortex along one edge and the inner wall lining along the other, and sits along the chord's length (C1); $\Theta = 90°$.

$$C1 = 2r\sin(\Theta / 2), \text{ or } 62.5 \text{ mm.} \quad (3)$$

For eighths, C1 was calculated the same way for $\Theta = 45°$; C1 = 16.91 mm. Dividing 62.5 mm by *t* (0.65 mm per strand) gave 96 'complete' strands between points *a* and *b*, or 384 for four similarly aligned quarters. For eighths there were 52 full wall strands, or 416 for the whole culm round. For quarters or eighth sections, the model produced one 8x or 16x repeatable set of 96 / 2 = 48, or 52 / 2 = 26 model strands from point *c* and X_1, respectively. The strand width ranged from a wall thickness of 11.05 mm at the *Y*-axis to a maximum of 14.28 mm (quarters) or 11.76 mm (eighths) at X_1. The x-axis values were calculated for quarters as,

$$X_{i1} = t, X_{i2} = 2t, X_{i3} = 3t, \ldots \text{ through to 48 at point } X_1 \text{ (31.2 mm)} \quad (4)$$

and for eighths, at point 26 (16.9 mm). The corresponding Y_i and y_i values, and strand widths were calculated using Eq. 2.

The two triangular-shaped edge sections (shaded) on each quarter or eighth round, located between points X_j and X_k in Figure 4b, gave an 8x repeatable set of 12 strands of decreasing thickness; for a total of 96 narrow strands. For eighths there was a 16x repeatable set of 6 narrow strands; similarly for a total of 96 narrow strands. The example calculations for strand width from the triangular edge portions are given below for quarters. In Fig. 4b the distance between X_1 and X_2 = (C2 – C1) / 2.

$$C2 = 2R\sin(\Theta/2), \text{ or } 78.135 \text{ mm} \quad (5)$$

Then, (C2 – C1) / 2 = 7.8175 mm, divided by 0.65 gave 12 strands. Starting at X_1, the *X*-axis values are,

$$X_{11} = X_1 + t,\ X_{12} = X_1 + 2t,\ X_{13} = X_1 + 3t,\ \ldots.\ \text{through to 12 at point } X_2\ (39.0\ \text{mm}) \quad (6)$$

the corresponding Y_i values for the 12 points between X_1 and X_2 are as follows:

$$Y_i = (R^2 - X_{1i}^2)^{½} \quad (7)$$

The actual strand width is $Y_i - Y$, and the Y values are for the 12 points along the line *b* to *e*. Because $\Theta / 2 = 45°$, $Y = X_{1i}$. The strand width decreased from X_1 and X_2, down to 1.0 mm for the last strand.

Strand contribution to transverse sectional area of culm wall

The model strands from each slicing configuration enables determination of the contribution of each strand to the total culm wall transverse cross-sectional area, *A*. This information helped explain why there were different numbers of strands generated for each slicing configuration. The transverse cross-sectional area of the entire 'model' culm wall is,

$$A = \pi R^2 - \pi r^2, \text{ or } 3452.3\ \text{mm}^2 \quad (8)$$

The transverse cross-sectional area of each individual strand (SA_i) in each model is $SA_i = 0.65\ W_i$, where W_i represents strand width (mm) at the mid-point of its thickness. The cumulative contribution of each strand ordered from largest to smallest could then be plotted and compared between slicing configurations.

Cortex exposure on strands

Every strand, both in practice and theoretically, has one edge (and in some cases one face) that is the hard waxy outer cortex, which adversely affects the resin bonding. The area of exposed cortex on the edge of each strand sliced in a given configuration can be calculated, and it will be different depending on whether the culm is sliced whole or halves, or as stacked quarters or eighths. The total length and area of outer cortex wall per full round is πD, or 347.15 mm, × L (130 mm) = 45128.2 mm^2. In a complete round, there are two edge strands that are cortex on one face, 34 strands that have cortex on both edges, and 272 strands with cortex on one edge. From Fig. 4a the angle Θ at point c is,

$$\Theta_i = \cos^{-1}((R - nt) / R) \quad (9)$$

where n is the number of strands from point R at the outer circumference, and t is the strand thickness (mm). The full segment length was calculated as,

$$S_i = R2\Theta_i \quad (10)$$

where Θ_i corresponds to the ith cumulative strand thickness increment from R. The segment length of cortex on the edge of a particular strand was calculated as,

$$S_i - S_h \quad (11)$$

where S_h is the full segment length (mm) for the preceding strand located at the point R – (nt - 0.65) out from c along the X-axis.

The total area of cortex remains the same if two halves are sliced. However, there are four strands with a cortex on one face, no strands with a cortex on both edges, and a total of 340 strands that have a cortex on one edge. The segment length of each quarter round was 86.86 mm, and there was a total of 120 strands per quarter, none of which had

cortex on one face or both edges. The list of all strands generated from one culm round in each cutting configuration with their calculated area of cortex was derived.

RESULTS AND DISCUSSION

The strand width distributions from physically stranding whole culm rounds, half culm rounds, and quarter culm rounds are shown in Fig. 5a, and the width distributions for model strands sliced as whole culm rounds, half culm rounds, quarter culm rounds, or eighths are shown in Fig. 5b.

The slightly bi-modal distribution found in the measured strands from whole culms was also seen in the shape of the model strand frequency distribution. The models predicted that no strands generated from slicing full rounds would be less than 10 mm in width, and none less than 5 mm in the case of slicing half rounds. In contrast, no model strands generated from stranding quarters or eighths were greater than 20 mm in width, despite there being strands wider than this when sampling the real strands. Note that there were also fewer strands in the 15 to 20 mm width class than predicted by the model for quarters. These discrepancies between predicted and actual counts are caused by greater mis-alignment of quarters in the strander draw compared with the perfect alignment (see Fig. 2). Also, during stranding, no matter what the size and shape of the culm pieces, there were always very narrow slivers (known in the OSB industry as 'fines') produced, and strand breakage caused by damage to the tissue during slicing and handling.

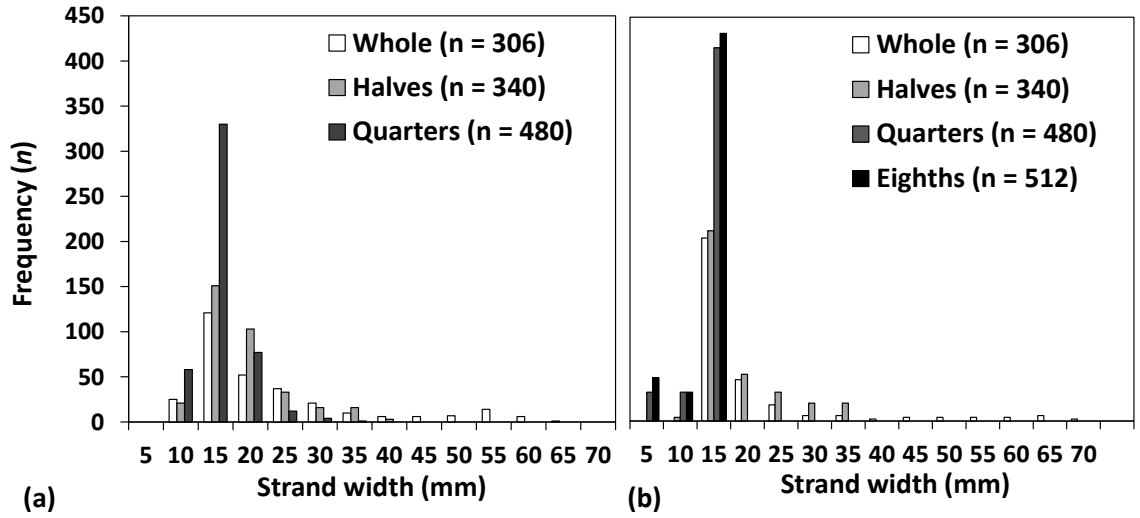

Fig. 5. (a) Observed and (b) model strand width distributions of stranding a whole round, 2 half rounds, 4 quarters, or 8 eighths at nominal target thickness = 0.65 mm

The amount of fines and dust generated during stranding would also increase greatly if the material has partially dried between harvesting/transport and the processing plant, and in practice, moisture content of the tissue at time of processing may be much lower than used here, and also much more variable. Therefore, it should be noted that the model made the assumption that all slices were perfectly clean and that none of the strands fragmented during slicing and handling. The screening of the strands through a

14.7-mm sieve was to remove the very fine slivers (< 5 mm) and dust, and therefore no pieces < 5 mm in width were sampled in the distribution for real strands.

The numbers of real strands measured from stranding full rounds, halves, or quarters matched to the number model strands generated from slicing one culm round, (Table 2). Table 2 also gives the percentage occurrence of different size classes of both model and real strands and average area of cortex per strand calculated in each model. Stranding one whole round in 0.65 mm increments produced a total of 306 model strands, 274 (89.5%) of which were above 10 mm in width. Stranding one round in the form of two stacked half rounds produced 340 strands, 316 (93%) were > 10 mm wide. Stranding one culm round in the form of four stacked quarter rounds produced 480 strands, 416 (86.7%) were > 10 mm wide; and stranding 8 eighth sections gave 512 strands, 432 (83.7%) were more than 10 mm wide. If the culm were to be fully radial sliced (which was not practical in reality) such that the outer edge of each strand was 0.65 mm, then a total of 534 strands would be produced from the 'model' culm. A visual comparison of the four models for strand width ordered from highest to lowest is shown in Fig. 6a, and the cumulative strand width in Fig. 6b.

Table 2. Strand Size Classification and Cortex Exposure Calculated for the Four Model Configurations

Culm Piece Size	Total Strands	Average Width (mm)	No. > 10 mm	Average Cortex Area (mm^2)	% Fines (< 10 mm)	% Optimum Strands (10 mm to 30 mm)	% Wide Strands (> 30 mm)
Model Strands							
Whole	306	17.4	274	147.5	0	89.5	10.5
2x Halves	340	15.6	316	132.7	1.2	92.9	5.9
4x Quarters	480	11.1	416	97.4	13.3	86.7	0
8x Eighths	512	10.2	432	87.6	15.6	84.4	0
Real Strands							
Whole	306	20.6	282	na	8.0	75.7	16.3
Halves	340	16.4	319	na	6.2	88.3	5.5
Quarters	480	12.9	413	na	13.9	86.1	0

From Table 2 and Fig. 6a, slicing halves generated the highest proportion of strands that measured 10 mm to 30 mm wide (93%); despite the lower total strand number, a trend also found in sampling the actual strands. There was also a greater occurrence of wide strands > 30 mm sampled in the real strands, which probably reflected some sampling error, size and shape irregularity, and variability in wall thickness in the real culms. As the culm was divided into narrower sections, the complete strands became closer to one fixed narrow width (Fig. 6a). Slicing whole rounds resulted in the occurrence of almost 10% of 'post card' strands, which were excessively wide strands (> 35 mm) that were prone to curl during drying. A more consistent strand width reduced the occurrence of fines and curled strands, reduced mat bulk density, and allowed for better strand alignment during OSB production and resulted in better board properties.

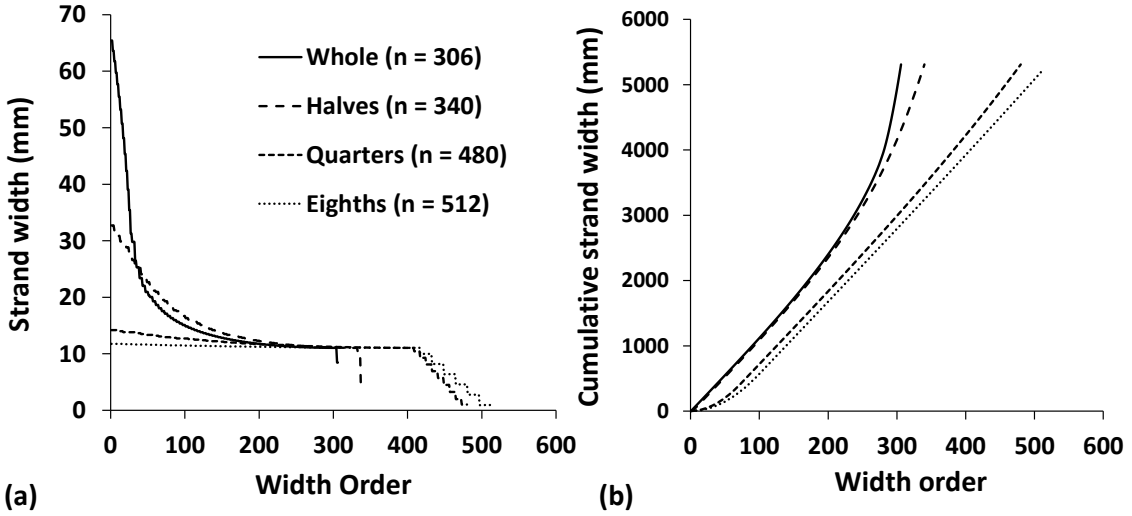

Fig. 6. (a) Strand width distribution and (b) cumulative strand width for model strands ordered from widest to narrowest from slicing whole culm, 2 halves, 4 quarters or 8 eighths

However, all of the strands should also not be too narrow; in industrial OSB manufacture the most effective strand alignment occurs for strand widths between 15 mm and 35 mm, aspect ratios (length/width) between 3 and 10 (Chen *et al.* 2008). This means that all of the strands cut from quarters or eighths were just below the lower recommended width for industrial OSB strands. Strands less than 10 mm wide were therefore classified as 'narrow strands' or 'fines', many of which may have been removed during screening through a 14.7 mm screen, which was done for the real strands to better reflect likely width distribution in screened industrial OSB strands. In reality, not all the 'fines' are removed, and a portion end up in the furnish used to manufacture OSB. If the authors were to fully discount the < 10 mm strands as being completely removed during screening, conversion to quarters and eighths would produce 36.6% and 57.7%, respectively, more strands > 10 mm in width than if the culm rounds were stranded whole. A slight increase in the average width of Moso strands, perhaps from stranding as halves, or perhaps even thirds, or thicker walled culms, with the same high recovery rate would be desirable. An increase in the culm diameter and wall thickness would increase the total numbers of strands sliced per culm round and *vice versa*. Also, that the increase in strand numbers from conversion to quarters or eighths may vary only slightly, if at all, over a realistic range of culm sizes (*e.g.* 50 mm to 150 mm diameter and 5 mm to 15 mm wall thickness). Clearly, the optimal culm stock for conversion to quarters/eighths and stranding will have thicker walls and a larger diameter so that both the width of the sections and the widths of each strand will be maximized. It could be hypothesized that the increase in numbers of strands from converting and slicing quarters and eighths may increase slightly if the culm diameter increased. These effects are of great interest to improve the practical validity of the model. However, time constraints did not permit further development of the model to run additional iterations of culm dimensions, to check the sensitivity of the model to changes in culm diameter and/or wall thickness. Other useful further investigation would be to develop a theoretical consideration of the slicing of stacked bamboo quarters or eighth sections through a curved plane as occurs in a ring strander. This may also help artificially boost average strand width for a given wall thickness.

Note from Table 2 and Fig. 5, the percentages of strands in each size class for real strands were close to the figures for model strands, particularly in the case of quarters. For real strands there was a greater occurrence of narrow strands less than 10 mm than in the model predictions for stranding whole culm or halves. This was likely due to variability in diameter and wall thickness of the stranded culm stock, which ranged from 83 mm to > 120 mm in diameter and from 8 mm to > 15 mm in wall thickness, while the model used one fixed diameter and wall thickness for demonstration purposes. During production of real strands many of the pieces were not perfect in shape or contained splits, and the orientation of the pieces in the feed draw was an approximation of the perfect theoretical packing and alignment (Fig. 2). During mechanical sieving of the real strands not all of the narrow strands were removed either.

As the width of the stranded pieces decreased from whole/half to eighths the proportion of narrow strands (< 10 mm wide) increased, and the fraction of 'optimum' strands decreased to 84.4% for eighths. Figure 7a shows the cumulative percentage of strands narrower than the maximum possible width of 65.45 mm (whole culms) for each model. For quarter and eighth sections there is a marked increase in the cumulative percentage of strands < 11 mm wide due to the very small strands from the shaded zones shown in Fig. 4b. Of these 96 narrow, or 'partial wall' strands produced from quarters or eighths, the greater proportion of these were very narrow in the case of eighths. Average width of these was 5.5 mm compared with 7.0 mm for quarters. Figures 7b to 7c overlay the cumulative % narrower distributions predicted for slicing the model culm with those found from sampling the real strands for whole, 2 halves, or 4 quarters, respectively. The model distributions generated from the average real culm dimensions closely matched the real strand distributions. Note from Table 2 that the average width of the real sampled strands (20 mm, 16 mm, and 13 mm for whole, halves, or quarters) were higher than those of the model strands (17 mm, 15 mm, and 11 mm, respectively). This discrepancy likely stemmed from a variety of factors that included the actual rounds being slightly larger in their dimensions than those used in the model, imperfectly shaped rounds, imperfect piece alignment during slicing, and sampling error.

Figure 8a shows the cumulative transverse culm wall area occupied by the strands in order from widest to narrowest, *i.e.* the area occupied by one end of each strand as a proportion of the total area of solid culm wall in a cross-section. Total transverse cross-sectional area was reached over fewer individual strands from slicing whole culms, and over a greater number of smaller strands for quarters and eighths. Eighths produced the highest proportion of strands of consistent width (Fig. 5a); but it should be noted no strands were wider than 11.8 mm, which meant the total culm wall transverse area was divided over a greater number of strands. Cumulative cross-sectional area of culm wall occupied by strands helped to explain how converting the culm rounds to quarters or eighths and slicing as much in the radial direction as possible generated more strands per unit volume of solid culm stock than simply slicing rounds or halves. For the whole or halves, the higher slope near intercept indicated the wider strands and their greater area contribution per strand.

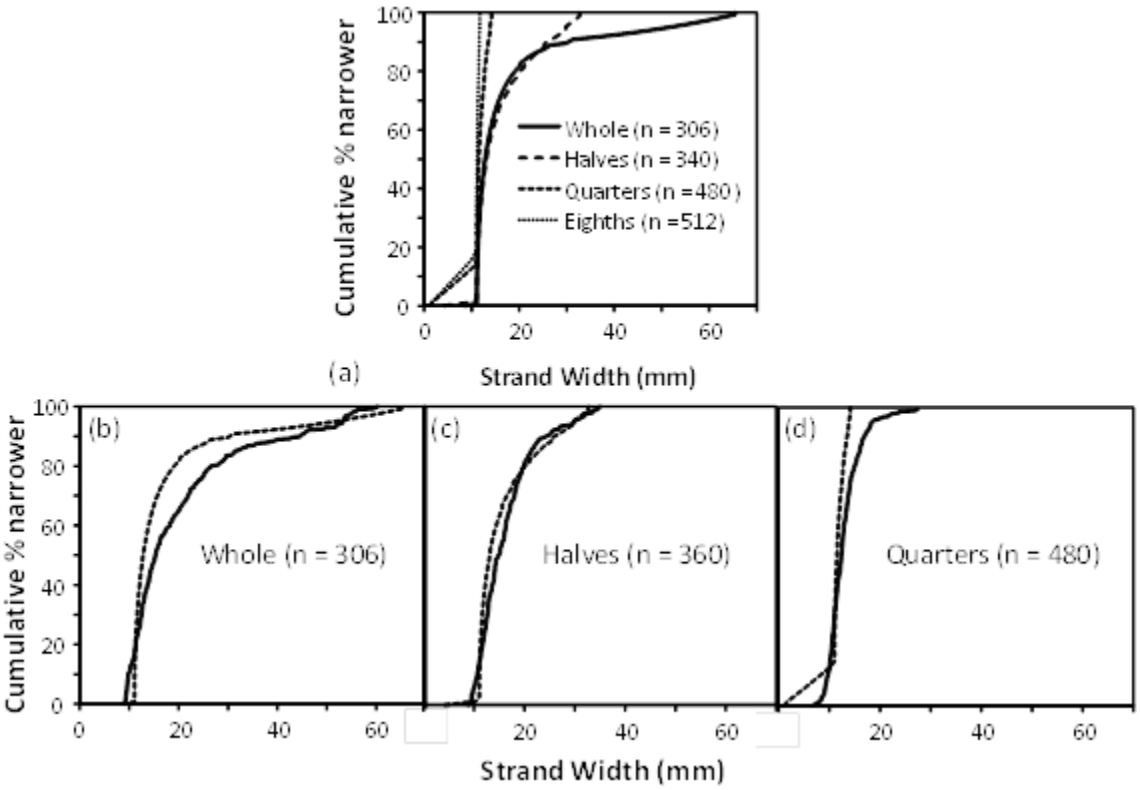

Fig. 7. (a) Cumulative % narrower distributions for model strands ordered from narrowest to widest; (b), (c), and (d) cumulative % narrower distributions for real *vs.* model predictions for slicing a whole round, 2 halves, or 4 quarters, respectively

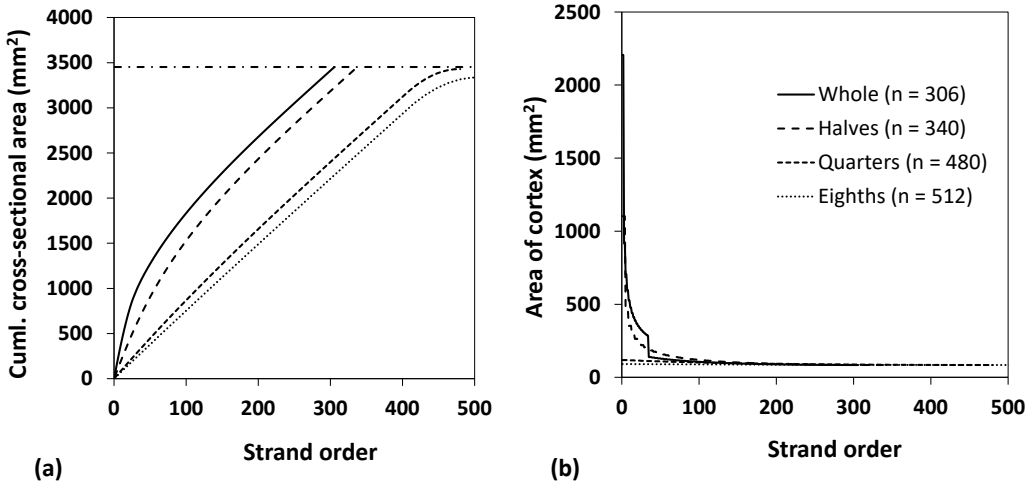

Fig. 8. Strand ordered smallest to largest (a) Cumulative transverse area contribution of strands; b) area of outer cortex of strands ordered from largest to smallest from slicing whole culm, two halves, 4 quarters, or 8 eighths

Figure 8b shows the area of hard, waxy outer cortex on all of the model strands ordered from highest to lowest, and the average cortex areas on strands in each model are listed in Table 2. Exposed waxy bamboo cortex on strands interferes with resin bond formation, creating weak zones or flaws in strand products that fail first under tensile

stress (Semple *et al.* 2015c, d). The models showed very low, and very little difference in cortex exposure between slicing quarters or eighths. For whole or two halves there was a small number of strands with high cortex exposure area, and also relatively little difference between slicing whole or two halves. The sudden decrease in cortex area per strand for whole rounds marked the transition from the outer two zones where each strand had cortex on both edges, to the inner wall after which each strand had cortex on just one edge. As a reference, the total area of outer cortex in the uncut culm was 45,129 mm^2, with a corresponding minimum area of cortex per strand if they were to be cut fully radially, of 84.5 mm^2. The two strands cut closest to the y axis had 84.5 mm^2 of cortex, and increased with every successive strand out towards *R* on the *x* axis. The maximum area of cortex on the two edge strands from slicing whole culms was 2,205.6 mm^2; the average area was 147.5 mm^2. The maximum area on the two edge strands for half culms was 1,102.8 mm^2 and there were four strands per round with this area of cortex on one face. The average area was 132.7 mm^2. For slicing quarters, the maximum area of cortex was 118.3 mm^2, for those strands located at points *d* and *e* (Fig. 4b); average area was 97.4 mm^2, and for slicing eighths the maximum area of cortex was 91.0 mm^2; the average area was 87.6 mm^2.

Whether round culms were stranded whole or converted to smaller pieces would make a difference to the machine efficiency of the strander, *i.e.* how many strands produced per knife revolution or running time. Conversion to quarters (or eighths if they could be tightly secured during stranding) and close stacking produced more strands per knife revolution. Per knife revolution there was either 1 or 2 strands per culm round (Fig. 2a), 2 strands per culm round for stranding halves (or 4 in Fig. 2b), and 4 per culm round for stranding quarters, which equated to the number of strands cut per knife revolution. Due to more efficient stacking in the feed drawer and less air space between pieces, up to 10 to 12 strands could be cut per knife revolution. This meant that to produce the same number of strands, the strander running time and energy costs could be cut by up to $1/6^{th}$ by splitting the rounds into quarters and using tightly stacked culm pieces.

The strand production method used in this study was by necessity laboratory scale only, and every effort was made to ensure the culm tissue was fully saturated to ensure clean slicing of full-sized strands. In an industrial setting, either diameter disk stranders (capable of cutting tissue longitudinally or cross-grain) or ring stranders (cross-grain only) would be used to produce strands form long poles or flitches of bamboo. In addition the flitches are also likely to be quite variable in their moisture level at the time of processing, with drier material leading to greater fragmentation of strands, and dust and fines production. Some greater deviation of sampled strand width distributions in this case from the model predictions would be expected. The orientation of the material relative to the knife (slicing along or across the grain) is not expected to affect the strand numbers or width distribution. However, the width distribution of strands would be altered if using a ring flaker, because the slices are cut through a curved plane. Bamboo culm processing factories in China have simple motorized corers fitted with wagon-wheel-shaped splitting cones that quickly and efficiently complete the task of splitting fresh green culm poles, (usually in 8 ft lengths) into any desired number of even-sized sections while pushing out the node plates during the process. This method was used by Fu (2007b) to convert culms to eight narrow sections in preparation for stranding and this study proved numerically that this substantially increased strand recovery compared with nesting and slicing whole rounds.

CONCLUSIONS

1. As the number of sections per round increased and were stacked for slicing, the recovery of strands per unit volume of culm could be increased by over 50%. However, this came at the expense of range across strand widths and an absence of strands greater than 14 mm wide in the case of quarters, or 12 mm in the case of eighths.
2. Conversion to halves, quarters, or eighths reduced or eliminated the occurrence of 'post-card' strands wider than approximately 35 mm, which were prone to curling.
3. The proportion of fines (strands < 10 mm in width) increased for quarters and eighths.
4. The shape of the frequency distributions for both real measured and model strand widths that resulted from slicing whole culm was slightly bi-modal. Another small peak occurred in the upper range of strand widths (> 50 mm).
5. Percentage frequency (expressed as cumulative % narrower) distributions found in real strands were fairly reliably predicted by the model slicing configurations for whole, halves, or quarters.
6. Conversion to quarters or eighths greatly minimized the area of exposed outer cortex, and was also far more efficient in terms of strander running time, *i.e.* number of strands cut per knife revolution.
7. Although recovery was lower, the desired range of strand width for OSB manufacture (approximately 15 mm to 35 mm) was best met by slicing strands into halves. Strand width for radially cut quarters, and certainly eighths with a culm wall thickness of 11 mm, was below the optimum range of widths for OSB.

ACKNOWLEDGEMENTS

The authors would like to acknowledge the following people and organizations: NSERC (National Science and Engineering Research Council); G8 Tri-Council grant for UBC, MIT and University of Cambridge; Mr. John Hoffman, Senior Technician at FPInnovations (Western Division), Vancouver, BC, for strander operation; Mr. Martin Smola, Undergraduate Applied Science co-op student, Fachhochschule Rosenheim, Germany, for assistance with strand production and measurement; and Mr. Keith Russell, UBC Department of Civil Engineering Co-op Program for advice and independent verification of models.

REFERENCES CITED

Anon (2012). "Aiming for domination," *Wood Based Panels International Online*, (http://www.wbpionline.com/features/aiming-for-domination/), Accessed 10 April 2013.

Austin, R., and Ueda, K. (1972). *Bamboo*, Weather Hill Publishing, New York, pp. 211.

Carmanah Design and Manufacturing Inc. (2006). *6/36 Lab Flaker Technical Manual*, Carmanah Design and Manufacturing Inc., Vancouver, BC.

Chen, S., Du, C., and Wellwood, R. (2008). "Analysis of strand characteristics and alignment of commercial OSB panels," *Forest Prod. J.* 58(6), 94-98.

Clouston, P. L., and Lam, F. (2002). "A stochastic plasticity approach to strength modeling of strand-based wood composites," *Compos. Sci. Technol.* 62, 1381-1395. DOI: 10.1016/s0266-3538(02)00086-6

Correal, J. F., and Ramirez, F. (2010). "Adhesive bond performance in glue line shear and bending for glued laminated *Guadua* bamboo," *J. Trop. Forest Sci.* 22(4), 433-439.

De Flander, K., and Rovers, R. (2009). "One laminated bamboo-frame house per hectare per year," *Constr. Build. Mater.* 23(1), 210-212. DOI: 10.1016/j.conbuildmat.2008.01.004

Dixon, P. G., Malek, S., Semple, K. E., Zhang, P. K., and Smith, G. D. (2017). "Multiscale modelling of moso bamboo oriented strand board," *BioResources* 12(2), 3166-3181. DOI: 10.15376/biores.12.2.3166-3181

Fu, W. (2007a). "Bamboo-a potential resource of raw material for OSB in China," *China Forest Prod. Ind.* 34, 21-24.

Fu, W. (2007b). *A Study on Flaking Technique and Manufacture of Bamboo OSB*, PhD Dissertation, Northeast Forestry University, Harbin, China, pp. 86.

Grossenbacher, M. (2012). "Industrielle Herstellung von Bambus-OSB: Ein Erfahrungsbericht [Industrial manufacturing of bamboo OSB: A review]," in: *2nd Bieler Holzwerkstoff-Workshop*, Biel, Switzerland.

Harries, K., Sharma, B., and Richard, M. (2012). "Structural use of full culm bamboo: The path to standardization," *Int. J. Arch. Eng. Constr.* 1(2), 66-75. DOI: 10.7492/ijaec.2012.008

Liese, W. (1998). *The Anatomy of Bamboo Culms*, Brill Academic Publishers, Beijing, China, pp. 175-191.

Lowood, J. (1997). "Chapter 5 Oriented strand board and waferboard," in: *Engineered Wood Products: A Guide for Specifiers, Designers and Users*, S. Smulski (ed), FPS Research Foundation, Madison, WI, pp. 123-145, +245.

Malanit, P., Barbu, M. C., and Fruhwald, A. (2011). "Physical and mechanical properties of oriented strand lumber made from an Asian bamboo (*Dendrocalmus asper* Backer)," *European J. Wood Prod.* 69(1), 27-36. DOI: 10.1007/s00107-009-0394-1

Malek, S., Zobeiry, N., Gereke, T., Tressou, B., and Vaziri, R. (2014). "A comprehensive multi-scale analytical modelling framework for predicting the mechanical properties of strand-based composites," *Wood Sci. Technol.* 49 (1), 59-81. DOI: 10.1007/s00226-014-0682-8

Moses, D. M., and Prion, H. G. (2004). "Stress and failure analysis of wood composites: A new model," *Compos. Part B-Eng.* 35, 251-261. DOI: 10.1016/j.compositesb.2003.10.002

Scurlock, J. M., Dayton, D. C., and Hames, B. (2000). "Bamboo: An overlooked biomass Resource?," *Biomass. Bioenerg.* 19, 229-244. DOI: 10.2172/754363

Semple, K. E., Smola, M., Hoffman, J., and Smith, G. D. (2014). "Optimising the stranding of Moso bamboo (*Phyllostachys pubescens* Mazel) culms using a CAE 6/36 disk flaker," M. Barnes and V. Herian, (eds), in: *Proc. 57th International Convention of Society of Wood Science and Technology*, Zvolen, Slovakia, pp. 257-269.

Semple, K. E., Zhang, P. K., Smola, M., and Smith, G. D. (2015a). "Comparison of stranding and strand quality of two giant timber bamboo species; Moso (*Phyllostachys pubescens* Mazel) and Guadua (*Guadua angustifolia* Kunth) from a CAE 6/36 disk flaker. Part I Tissue characterization, strand production and size classification," *BioResources* 10(3), 4052-4064. DOI: 10.15376/biores.10.3.4048-4064

Semple, K. E., Zhang, P. K., and Smith, G. D. (2015b). "Comparison of stranding and strand quality of two giant timber bamboo species; Moso (*Phyllostachys pubescens* Mazel) and Guadua (*Guadua angustifolia* Kunth) from a CAE 6/36 disk flaker Part II Surface classification and roughness indices," *BioResources* 10(3), 4599-4612. DOI: 10.15376/biores.10.3.4599-4612

Semple, K. E., Zhang, P. K., Smola, M., and Smith, G. D. (2015c). "Hybrid oriented strand boards made from moso bamboo (*Phyllostachys pubescens* Mazel) and aspen (*Populus tremuloides* Michx.): Uniformly mixed single layer uni-directional boards," *European J. Wood Prod.* 73(4), 515-525. DOI: 10.1007/s00107-015-0913-1

Semple, K. E., Zhang, P. K., and Smith, G. D. (2015d). "Hybrid oriented strand boards made from moso bamboo and aspen: Species-separated three-layer boards," *European J. Wood Prod.* 73(4), 527-536. DOI: 10.1007/s00107-015-0914-0

Starke, N. M., Cai, Z., and Carll, C. (2010). *Wood-based Composite Materials, FPL Wood Handbook, Centennial Edition*, (Report No. 190)," U.S. Department of Agriculture Forest Products Laboratory, Madison, WI.

Sumardi, I., Suzuki, S., and Ono, K. (2006). "Some important properties of strandboard manufactured from bamboo," *Forest Prod. J.* 56(6), 59-63.

Sumardi, I., Ono, K., and Suzuki, S. (2007). "Effect of board density and layer structure on the mechanical properties of bamboo oriented strandboard," *J. Wood Sci.* 53(6), 510-515. DOI: 10.1007/s10086-007-0893-9

Sumardi, I., Kojima, Y., and Suzuki, S. (2008). "Effects of strand length and layer structure on some properties of strandboard made from bamboo," *J. Wood Sci.* 54(2), 128-133. DOI: 10.1007/s10086-007-0927-3

Sumardi, I., and Suzuki, S. (2013). "Parameters of stand alignment distribution analysis and bamboo strandboard properties," *BioResources* 8(3), 4459-4467. DOI: 10.15376/biores.8.3.4459-4467

Triche, M. H., and Hunt, M. O. (1993). "Modelling of parallel-aligned wood strand composites," *Forest Prod. J.* 43(11/12), 33-44.

Van der Lugt, P., Van den Dobbelsteen, A., and Janssen, J. (2006). "An environmental, economic and practical assessment of bamboo as a building material for supporting structures," *Constr. Build. Mater.* 20(9), 648-656. DOI: 10.1016/j.conbuildmat.2005.02.023

Wang, Y. T., and Lam, F. (1998). "Computational modeling of material failure for parallel-aligned strand based wood composites," *Comp. Mater. Sci.* 11(3), 157-165. DOI: 10.1016/s0927-0256(97)00214-0

Article submitted: February 24, 2017; Peer review completed: June 18, 2017; Revised version received and accepted: August 22, 2017; Published: September 7, 2017.
DOI: 10.15376/biores.12.4.7841-7858